ISSN 1810-2328, Journal of Engineering Thermophysics, 2016, Vol. 25, No. 4, pp. 509–519. © Pleiades Publishing, Ltd., 2016.

Laminar Free Convection Heat Transfer Between Vertical Isothermal Plates

V. I. Terekhov[1,2*], A. L. Ekaid[3], and K. F. Yassin[2,4]

[1] *Kutateladze Institute of Thermophysics, Siberian Branch, Russian Academy of Sciences, pr. Akad. Lavrent'eva 1, Novosibirsk, 630090 Russia*

[2] *Novosibirsk State Technical University, pr. K. Marksa 20, Novosibirsk, 630092 Russia*

[3] *University of Technology, Baghdad, Iraq*

[4] *Technical Institute Hawija, Northern Technical University, Kirkuk, Iraq*

Received June 8, 2016

Abstract—The paper represents results on numerical investigation of flow and heat transfer between two isothermal vertical plates under laminar natural convection. A system of complete Navier–Stokes equations is solved for a two-dimensional gas flow between the plates along with additional rectangular regions (connected to inlet and outlet sections), whose characteristic sizes are much greater than the spacing between the plates. The calculations were performed over very wide ranges of Rayleigh number $\mathrm{Ra} = 10 \div 10^5$ and a relative channel length $\mathrm{AR} = L/w = 1 \div 500$. The influence of the input parameters on the gas-dynamic and thermal structure of thermogravitational convection, the local and mean heat transfer, and also the gas flow rate between the plates (convective draft. We determined sizes of the regions and regime parameters when the local heat flux on the walls tends to zero due to the gas temperature approach to the surface temperature. It is shown that the mean heat transfer decreases as the relative channel length AR grows, whereas the integral gas flow rate (convective draft) and Reynolds number in the channel $\mathrm{Re} = 2wUm/\nu$ increase. The use of a modified Rayleigh number $\mathrm{Ra}^* = \mathrm{Ra} \cdot (w/L)$ (Elenbaas number) leads to generalization of calculation data on mean heat transfer. These data are in good agreement with the correlations for heat transfer [1, 2] and gas flow rate [3]. The reasons of variation of the data in the range of low Rayleigh numbers are discussed in detail.

DOI: 10.1134/S1810232816040081

INTRODUCTION

The study of natural convection in vertical channels is important in many engineering applications, e.g., in cooling of electric and electronic equipments, in nuclear reactors, ventilation systems of buildings, and also in various power devices. To increase the efficiency of cooling of equipments and develop the fundamentals of free convection flows, an important stage is to conduct complex calculation investigations of new possibilities to intensify heat and mass transfer or increase the gas flow rate between the plates over a wide range of parameters.

Interest to this problem has aroused long ago. The problem on laminar and turbulent free convection between two parallel plates has become classical by now and is covered in a great deal of theoretical and experimental works among which we can mark [1–8]. With a small channel length the boundary layers develop independently on each wall and the flow is similar to natural convection on a vertical plate in an infinite volume. On the contrary, for long-length plates the boundary layers finally merge and the flow becomes fully developed. The use of superposition of these two limiting cases of the flow between the plates has allowed the authors of [1, 2] to obtain simple engineering formulas for determining the optimal spacing between the plates to attain the maximal gas flow rate or heat transfer.

However, further investigations [9–13] have shown that such limiting cases are not usually observed in the real conditions. A rough approximation is also the condition of equality of the pressure difference

* E-mail: terekhov@itp.nsc.ru

between inlet and outlet to buoyancy forces of temperature stratification without regard to the real gas density distribution both in height and width of the channel. All that considerably complicates the problem, hence, solving numerically the Navier–Stokes problem is in this case the most suitable method for analyzing the flow and heat transfer between the plates for both laminar and turbulent flows. Recently, interest to this problem is revived. This is caused primarily by requirements of practice for such significant devices as solar collectors, Trombe walls, ventilated facades of buildings. Understanding of the flow structure in elements of this equipments can significantly improve their construction and, hence, their operational characteristics.

STATEMENT OF THE PROBLEM. BOUNDARY CONDITIONS. SOLUTION PROCEDURE

A schematic of the problem is shown in Fig. 1. Two vertical plates with a height L were spaced at a distance w from each other. Their stretch parameter varied in the calculations in a wide range $\mathrm{AR} = L/w = 1 \div 500$. Temperatures of the plates was maintained constant and their values coincided $T_C = T_H = T_W$, so that the nonisothermality parameter characterizing the ratio of temperature differences on a hot wall and cold walls $R_T = (T_C - T_0)/(T_H - T_0)$ was $R_T = 1$. The ambient air temperature in the neighborhood of the inlet and outlet from the plates was the same and it was always lower than that of the walls, $T_0 < T_W$. Convective motion between the plates was due to thermogravitational forces caused by heating of the plates. The numerical solution was obtained for the case of free air convection with Prandtl number $\mathrm{Pr} = 0.71$. The Rayleigh number varied over a wide range $\mathrm{Ra} = 10 \div 10^5$.

The numerical investigations were performed via solving two-dimensional Navier–Stokes equations and an energy equation in Boussinesq approximation.

Continuity and momentum conservation equations:

$$\left(\frac{\partial U}{\partial X} + \frac{\partial V}{\partial Y}\right) = 0, \tag{1}$$

$$\left(U\frac{\partial U}{\partial X} + V\frac{\partial U}{\partial Y}\right) = -\frac{\partial P}{\partial X} + \sqrt{\frac{\mathrm{Pr}}{\mathrm{Ra}}}\left[\frac{\partial}{\partial X}\left(\frac{\partial U}{\partial X}\right) + \frac{\partial}{\partial Y}\left(\frac{\partial U}{\partial Y}\right)\right], \tag{2}$$

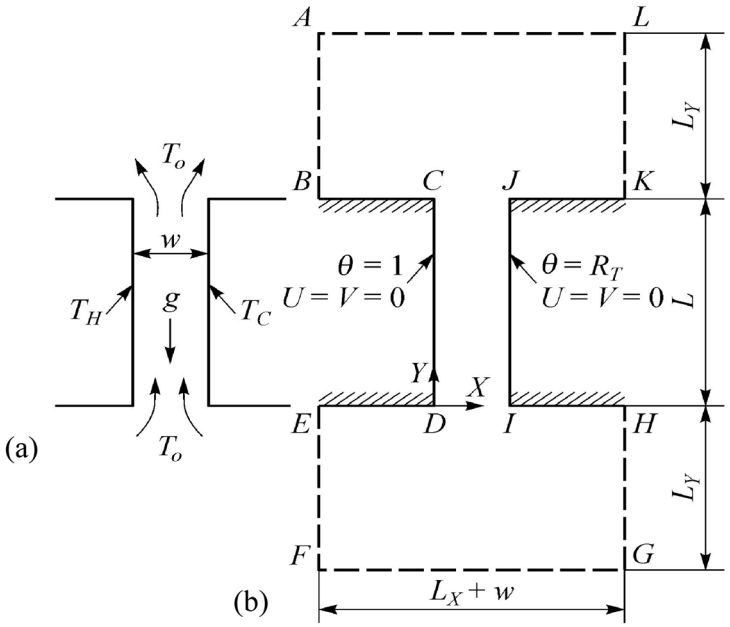

Fig. 1. (a) A schematic of the flow; (b) computation domain.

$$\left(U\frac{\partial V}{\partial X}+V\frac{\partial V}{\partial Y}\right)=-\frac{\partial P}{\partial Y}+\sqrt{\frac{\mathrm{Pr}}{\mathrm{Ra}}}\left[\frac{\partial}{\partial X}\left(\frac{\partial V}{\partial X}\right)+\frac{\partial}{\partial Y}\left(\frac{\partial V}{\partial Y}\right)\right]+\theta. \tag{3}$$

Energy conservation equation:

$$\left(U\frac{\partial \theta}{\partial X}+V\frac{\partial \theta}{\partial Y}\right)=+\frac{\partial P}{\partial Y}+\frac{1}{\sqrt{\mathrm{PrRa}}}\left[\frac{\partial}{\partial X}\left(\frac{\partial \theta}{\partial X}\right)+\frac{\partial}{\partial Y}\left(\frac{\partial \theta}{\partial Y}\right)\right]. \tag{4}$$

The system of equations (1)–(4) was solved in dimensionless form with the following variables:

$$\begin{gathered}X,Y=\frac{x,y}{w},\quad U,V=\frac{u,v}{u_{ref}},\quad P=\frac{p}{u_{ref}^2},\quad \theta=\frac{T-T_0}{T_H-T_0},\\ u_{ref}=\sqrt{g\beta(T_H-T_0)w},\quad \mathrm{Ra}=\frac{\rho^2 g\beta(T_H-T_0)w^2\mathrm{Pr}}{\mu^2},\quad \mathrm{Pr}=\frac{\nu}{\alpha},\quad A=\frac{L}{w}.\end{gathered} \tag{5}$$

The flow field parameters are characterized by Reynolds number

$$\mathrm{Re}=\frac{\rho V 2w}{\mu}=2V_m\sqrt{\frac{\mathrm{Ra}}{\mathrm{Pr}}}, \tag{6}$$

where V_m is the mean velocity between the plates,

$$V_m=\int_0^{-1}V\,dX. \tag{7}$$

The local Nusselt number is defined as:

$$\mathrm{Nu}_H=\left.\frac{\partial \theta}{\partial X}\right|_{X=0}, \tag{8}$$

and the mean Nusselt number along channel length is defined as:

$$\overline{\mathrm{Nu}}_H=\frac{1}{A}\int_0^A \mathrm{Nu}_H\,dY. \tag{9}$$

Thermal balance of the flow in the channel yields the following expressions for integral Nusselt number on both walls:

$$\overline{\mathrm{Nu}}_0=\frac{1}{A}\int_0^{-1}\left[\left(\mathrm{Pr}\sqrt{\frac{\mathrm{Ra}}{\mathrm{Pr}}}V\theta\right)_{Y=A}-\left(\mathrm{Pr}\sqrt{\frac{\mathrm{Ra}}{\mathrm{Pr}}}V\theta\right)_{Y=0}\right]dX. \tag{10}$$

The integral heat transfer value on both cold and hot plates was also found by summing up the heat fluxes by relation (9). At that, the difference between the results of calculation and thermal balance (10) was under 0.4%.

NUMERICAL METHOD

To discretize the governing equations we use the finite volume method. The system of algebraic equations is solved by a sweep method implicitly by a linear Gaussian elimination scheme. To approximate convection terms in the equations of motion and energy we used the reverse flow scheme. A computer program was designed to obtain numerical results using pressure–velocity conjugation (SIMPLE algorithm) [14]. Due to this rigid conjugation and nonlinearity of the equations, to provide convergence a relaxation procedure is needed. The relaxation multipliers are used for components of velocity, temperature, and pressure, 0.5, 0.8, and 0.7, respectively. To speed up convergence, the relaxation coefficients have to be chosen for each of the cases [14]. The convergence criterion in

Table

Boundary conditions	U	V	θ
AB and LK	$\partial U/\partial X = 0.0$	$V = 0.0$	$\partial\theta/\partial X = 0.0$
EF and GH	$\partial U/\partial X = 0.0$	$V = 0.0$	$\theta = 0.0$
FG	$U = 0.0$	$\partial V/\partial Y = 0.0$	$\theta = 0.0$
AL	$U = 0.0$	$\partial V/\partial Y = 0.0$	$\partial\theta/\partial Y = 0.0$
CD	$U = 0.0$	$V = 0.0$	$\theta = 1.0$
IJ	$U = 0.0$	$V = 0.0$	$\theta = R_T$
BC, DE, JK and HI	$U = 0.0$	$V = 0.0$	$\partial\theta/\partial Y = 0.0$

each of them was determined as $(\Phi_{i+1} - \Phi_i)/\Phi_i \le 10^{-5}$, where Φ is the independent variable under consideration and i is iteration number. In addition, the normalized remainders for the equations of mass, momentum, and energy conservation in the complete flow field have to be under 10^{-3}. For our calculations we developed a structured nonuniform mesh in Cartesian coordinates. To ensure accuracy of numerical results, we investigated the effect of mesh sizes on the calculated results. The calculation mesh size at the walls and in the inlet and outlet regions decreased by the power law. Between the plates in the main series of calculations we used a (30×60) mesh that, compared to a (60×120) mesh, yielded an error of less than 3% to provide accurate numerical results, the effect of the mesh sizes on the calculation results was investigated. The sizes of regions adjacent to inlet and outlet were also tested. The investigations have revealed that the optimal sizes of these regions are $Lx = (L + w)$ and $L_Y = L$. This issue is represented in more detail in [11, 12].

The boundary-value problem has unknown conditions at the inlet and outlet between the plates. For this reason, besides the space between the plates the calculation region includes two additional rectangles at the channel inlet and outlet with soft boundary conditions at the boundaries (Fig. 1b). The optimal size of the regions and the number of calculation nodes were determined in a series of numerical experiments and verifications on experimental data obtained in simpler conditions. As a rule, the linear size of the inlet and outlet regions was not smaller than the height of the plate L. Description of dynamic and thermal conditions at the boundaries is given in the table. The issue of testing the numeric code is represented in detail in [12, 15, 16].

RESULTS OF INVESTIGATIONS AND DISCUSSION

Figure 2 illustrates variation of longitudinal velocity and temperature along channel height at fixed values of Rayleigh number $\mathrm{Ra} = 1000$ and interlayer height $\mathrm{AR} = 10$. We should note that development of the flow is identical in many ways to a flow in a tube with the initial area being gradually transformed into a stabilized one. At that, due to formation of the vacuum space over the entire channel cross-section, in the wall region there is no velocity bend profile that is characteristic for free convection near a single vertical plate. In this case, already at the inlet section the velocity value near the axis reaches larger values.

At the channel outlet, as is clearly seen in Fig. 2a, the velocity profile becomes asymmetrical relative to the vertical axis. A possible reason of this behavior of the velocities is formation of a reverse flow due to reversal of external heavy liquid mass into the channel, as was noted in experiments and calculations of [5]. This is supported by results of the numerical investigations [12, 16]; however, this issue requires special study and does not be considered in the present paper.

Figure 2b illustrates the behavior of the profiles of dimensionless temperatures θ along the channel height. Development of the thermal field in the channel is demonstrated by computer visualization in Fig. 2c. For the considered conditions ($\mathrm{Ra} = 1000$ and $\mathrm{AR} = 10$) the temperature boundary layers merge even to $y/w \sim 2.5$ calibres and toward the channel outlet the flow becomes strongly heated and the temperature on the axis approaches its value on the wall.

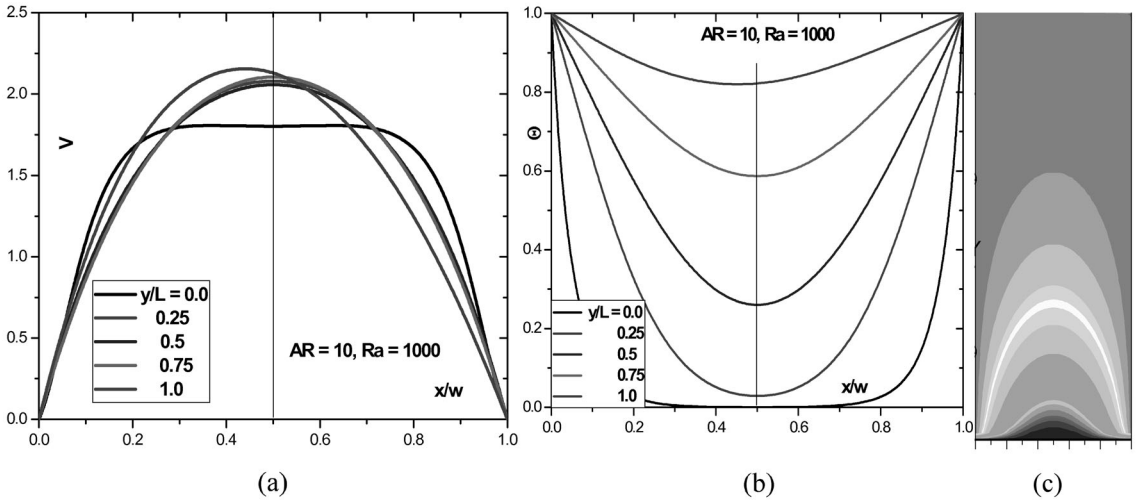

Fig. 2. Variation of (a) velocity and (b) temperature; (c) thermal visualization in channel height. AR = 10, Ra = 10^3.

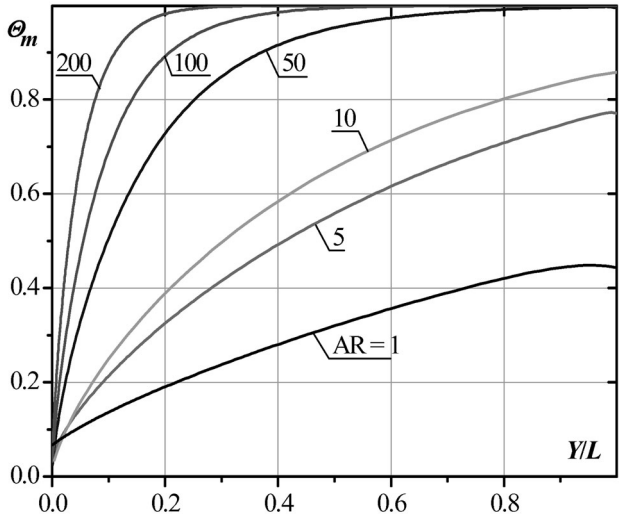

Fig. 3. Variation of bulk temperature for channels of different length. Ra = 1000.

The temperature field between the plates develops differently than the dynamic one. At the channel inlet its most part, except for wall regions, is occupied by a plateau with temperature of the environment, where $\theta = 0$. Then the flow is gradually heated so that its temperature becomes close to the value on the wall and $\theta \to 1$. This is illustrated in Fig. 2b. Thus, toward the channel outlet the heat flow from the wall to gas will decrease not only due to the growing thermal resistance of the boundary layer, but also due to the decrease in the temperature difference between the channel surface and gas.

Variation of the relative bulk temperature along channels of different length is illustrated in Fig. 3. For short channels (AR < 50) the ambient air has no time to heat up to the wall temperature, and the bulk temperature $\theta_m < 1$. As the channel length is increased, as follows from Fig. 3, increasingly more and more part of it does not participate in the heat transfer process. Really, at the considered Rayleigh number (Ra = 1000) the heat balance between the convective flow and the channel walls is attained approximately in the middle of the channel for AR = 100, at that, its other half is eliminated from the thermal process due to heating-up of the air. As the channel length is more and more increased, there occurs growth of the "ballast" part of the channel.

Figure 4 illustrates the distribution of longitudinal velocity at the outlet section of channels of different height. As the channel length increases more and more, the level of velocities increases due to growing

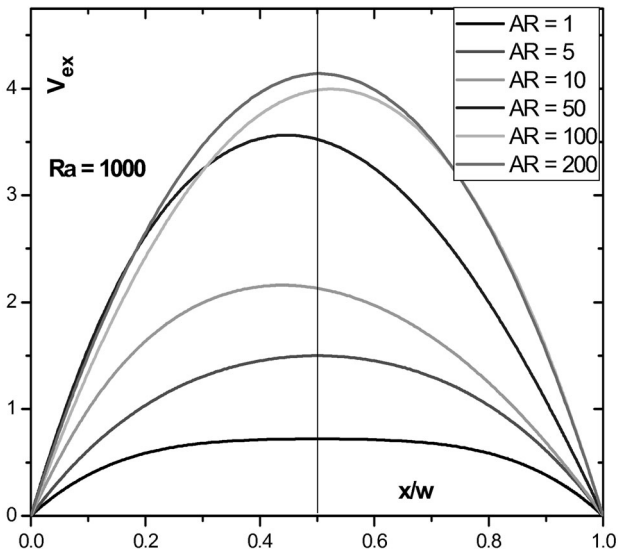

Fig. 4. Velocity profiles at the outlet with varying plate length. $\mathrm{Ra} = 10^3$.

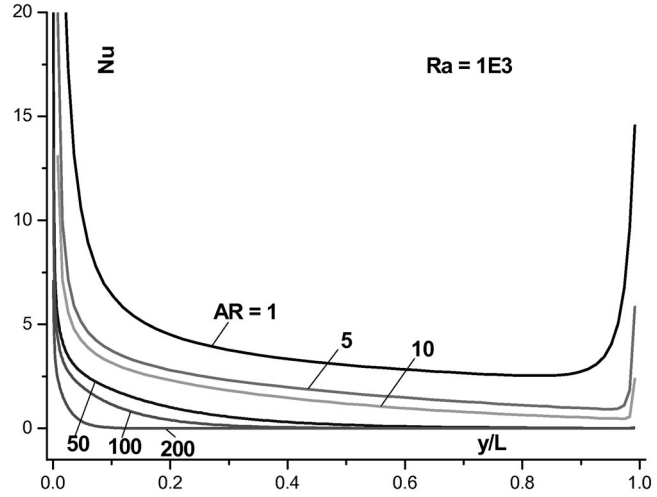

Fig. 5. Variation of the local Nusselt number along channels of different length. $\mathrm{Ra} = 1000$.

buoyancy forces whose value depends directly on the channel size. The calculations have shown that the flow becomes stable quite quickly and, beginning from $\mathrm{AR} > 5$, the velocity profiles become self-similar.

Figure 5 represents the calculation results as a variation of Nusselt number along channel height versus different values of the stretch parameter AR. It is seen that in channels of different height the number Nu changes more significantly; at that, for short channels the heat transfer intensity is considerably higher than for long ones. It is important that regions adjacent to channel outlet and inlet have a significant effect on the flow and heat transfer. In these zones, effects of flows around the channel rib result in detached vortex flows leading to heat transfer intensification.

By integrating the local distributions of the heat transfer coefficient, shown in Fig. 5, we have studied the behavior of mean heat transfer versus interlayer height and Rayleigh number. Such data are represented in Fig. 6a. As we should expect, the mean heat transfer grows with increasing Ra and considerably decreases for long-length channels. This is natural because the greatest part of short channels is occupied by boundary layers of small thickness; moreover, the gas temperature inside long channels rapidly reaches the wall temperature, hence the heat fluxes tend to zero. The greatest effect of the channel geometry (~ 3 orders of magnitude) is observed at low Rayleigh numbers.

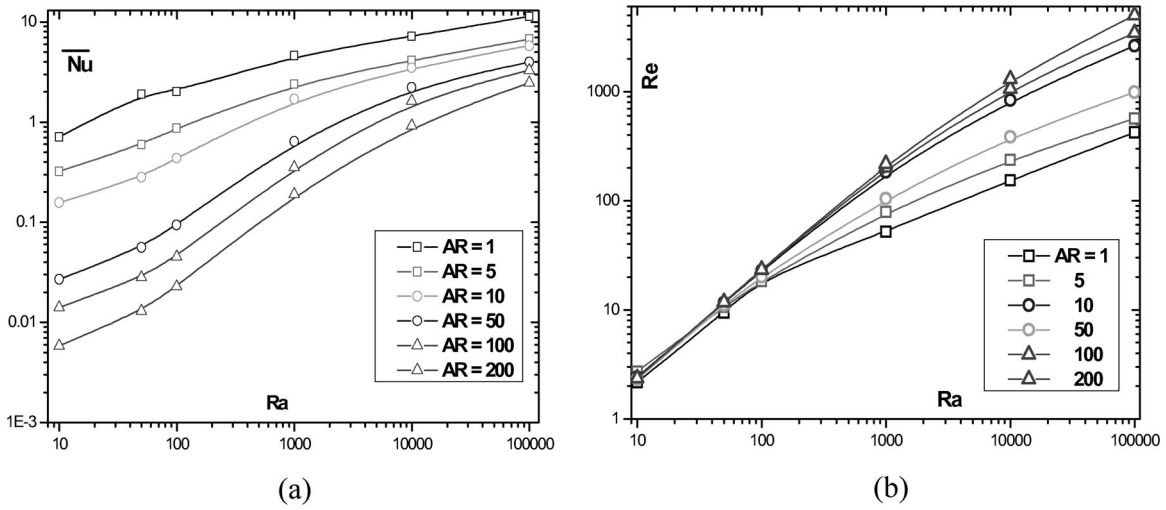

Fig. 6. Mean heat transfer (a) and Re number in the channel (b) versus Rayleigh number and the parameter AR.

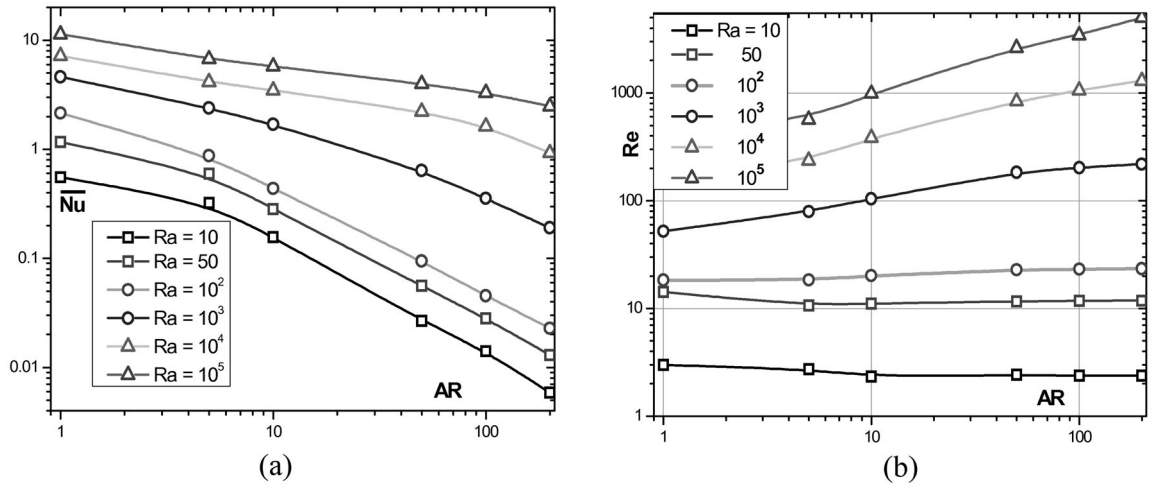

Fig. 7. Mean heat transfer (a) and Reynolds number (b) versus interlayer height.

The reverse situation is observed for gas flow rate inside the channel. This fact can be seen clearly in Fig. 6b, where the number $\mathrm{Re} = 2U_m w/\nu$ characterizes the gas flow rate in the interlayer and it does not change in the channel length. At low Rayleigh numbers the gas flow rate through the channel does not practically depend on its height, and as the parameter AR and the number Ra grow the air draft due to the buoyancy forces increases, which also corresponds to physics of the process.

The effect of the interlayer geometry on the heat transfer intensity and Reynolds number is most clearly demonstrated in Fig. 7. As Fig. 7a shows, the integral heat transfer decreases over the whole range of Rayleigh numbers as the channel length grows. However, the rate of the decrease in the range of high Rayleigh numbers is not as high as for low Ra. The explanation is the fact that a significant part of the log-length channels is occupied by the region with an extremely low heat transfer level (for example, see Fig. 5) while the size of the zone with efficient heat transfer remains practically the same for channels of different length.

The behavior of Reynolds number in the channel versus channel length is complicated (see Fig. 7b). At low Rayleigh numbers ($\mathrm{Ra} < 10^3$) the growth of thermogravitational forces due to increasing heat transfer surface is compensated for friction losses. For this reason, in this range of Ra numbers the gas flow rate through the channel does not practically depend on its height. Moreover, for small lengths

(AR < 10) it is first observed a slightly decreasing gas flow rate, but then it is stabilized. In the range of large Rayleigh numbers ($\mathrm{Ra} > 10^3$) the gas flow rate through the channel grows with increasing channel height, which evidences the predominant effect of the buoyancy forces versus friction. The mentioned peculiarities in the behavior of the thermal and dynamic characteristics with varying level of thermogravitational forces are important in optimization analysis of channels with parallel walls of different length.

MODIFIED RAYLEIGH NUMBER. GENERAL RESULTS

Generalizing the results of the numerical and physical experiments on heat transfer in vertical channels of different length, Elenbaas [1] was the first to use the modified Rayleigh number that considers the channel length scale:

$$\mathrm{Ra}^* = \mathrm{Ra} \cdot w/L. \tag{11}$$

Using the modified Rayleigh number Ra^*, Elenbaas [1] obtained the general expression for integral Nusselt number for channels of different length:

$$\mathrm{Nu}_{\mathrm{av}} = 1/24 \cdot \mathrm{Ra}^*[1 - \exp(35/\mathrm{Ra})^*]^{3/4}. \tag{12}$$

Bar-Cohen and Rohsenow [2] using the solution sewing method for free convection on the initial channel part and for a fully developed flow at a constant wall temperature have obtained the relation for integral heat dissipation in the function of modified Rayleigh number:

$$\mathrm{Nu}_{\mathrm{av}} = [576\mathrm{Ra}^{*2} + 2.83/\sqrt{\mathrm{Ra}^*}]^{-1/2}. \tag{13}$$

Results of the calculations by formulas (12) and (13) are represented in Fig. 8. The both dependences are sufficiently close to each other in a very wide range of Rayleigh numbers $\mathrm{Ra}^* = 10^{-2} \div 10^5$. The data of numerical calculations of the present work are also in good agreement. The results obtained for interlayers of all lengths at low Rayleigh numbers are the exception. A possible reason of such behavior of the heat transfer regularities is transition to asymptotic limit [13], which is observed at Rayleigh numbers tending to $\mathrm{Ra} \to 0$.

Figure 9 demonstrates variation of Reynolds number in channels of different length versus modified Rayleigh number. Contrary to the integral heat transfer, the use of Elenbaas parameter Ra^* does not lead to generalization of the calculation data and all the data are laminated depending on the channel height. And, as we should expect, in higher channels the air flow rate due to free convection grows.

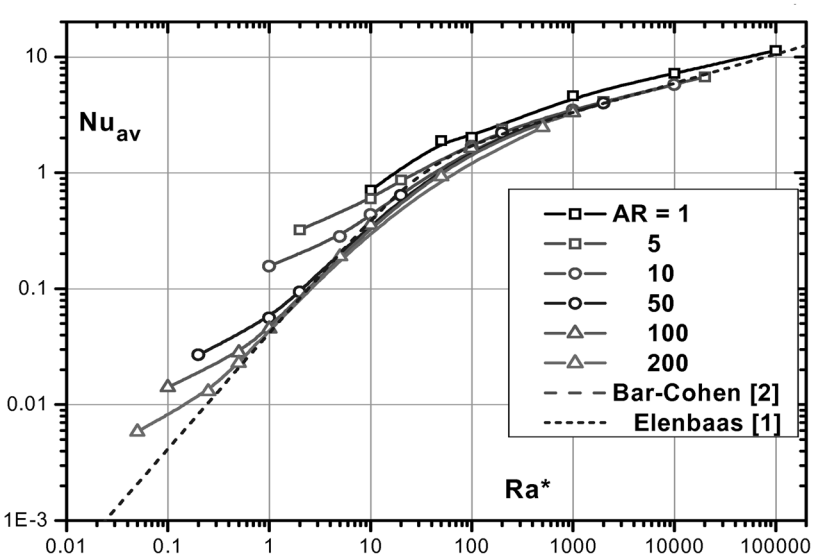

Fig. 8. Generalization of calculation data on mean heat transfer versus modified Rayleigh number Ra^*.

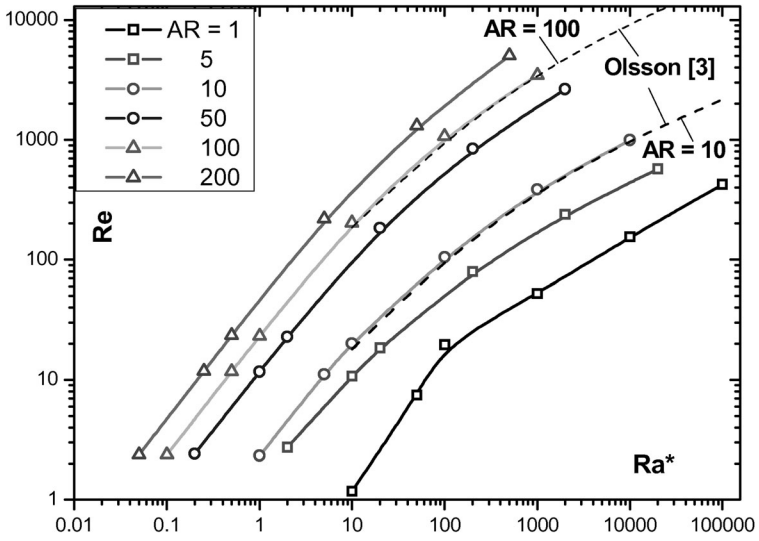

Fig. 9. The influence of Rayleigh number on the natural convective draft in channels of different length.

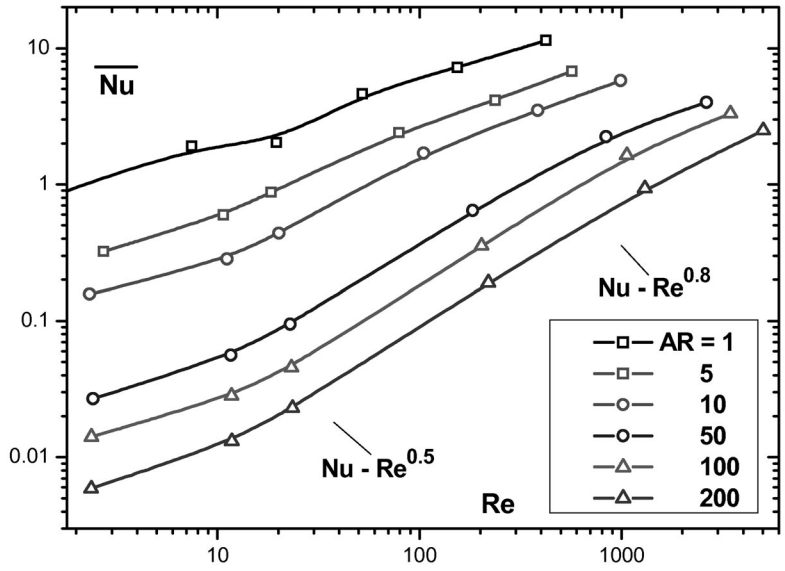

Fig. 10. Mean Nusselt number versus Reynolds number in vertical channels in the natural convection regime.

This fact was noted by Olsson in investigation [3], where the author performed detailed analysis and based on the method used in [2] for heat transfer obtained calculation relationships for Reynolds number for free laminar convection in a vertical channel with parallel walls. Under condition of a constant wall temperature the expression for Reynolds number looks as

$$\mathrm{Re} = 2/\mathrm{Pr} \cdot [(4\mathrm{Ra}^* \cdot \mathrm{Pr} \cdot \mathrm{AR}/f_{app})^{-0.405} + (6.6 \cdot \mathrm{Ra}^* \cdot \mathrm{Pr}^{1/4} \cdot \mathrm{AR}^{0.81})^{-1}]^{-1/0.81}, \qquad (14)$$

where f_{app} is the effective friction coefficient determined in [3] according to conclusions of the theory of laminar flow in ducts [17].

The results of calculations by formula (14) for the length parameters AR = 10 and 100 are represented in Fig. 9 by dashed lines. As it follows from the correlations, these lines absolutely agree with results of calculations of the present study over the whole range of Rayleigh number; this supports the possibility of using the approximate methods [3] for describing the hydrodynamics in vertical ducts in the regime of free convection.

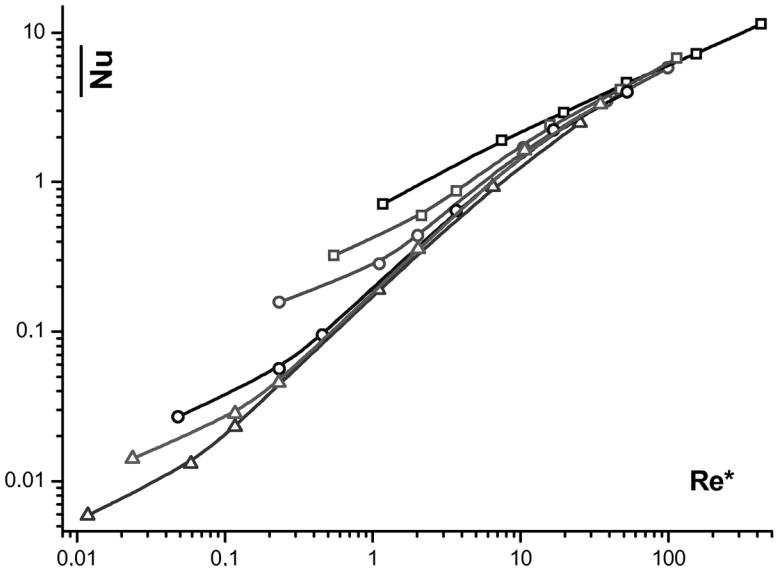

Fig. 11. Integral heat transfer in vertical channels versus modified Reynolds number. The designation correspond to Fig. 10.

The calculation data on mean heat transfer versus Reynolds number in the channel are represented in Fig. 10. Thereby all the obtained data were considered in terms of the forced convection laws regardless of the causes of convection flow. As is seen, in such processing, the calculation results obtained for channels of different length are not generalized. This behavior of the mean Nusselt number is explained by the presence of zones with lower heat transfer and by their different contribution to the integral heat transfer with varying channel length. Moreover, in Fig. 10, one clearly observes the regularity $\mathrm{Nu} \sim \mathrm{Re}^{0.5}$ in the region of low Reynolds numbers and $\mathrm{Nu} \sim \mathrm{Re}^{0.8}$ in the region of high ones, though this behavior of heat transfer has no bearing on the heat transfer.

Further attempts to generalize the data of the numerical investigation were based on using the modified Reynolds number. By analogy with Rayleigh number, the modified Reynolds number was calculated with regard to the interlayer stretch parameter $\mathrm{Re}^* = \mathrm{Re} \cdot (w/L)$. The use of such a parameter considerably groups the calculation data. This is seen in Fig. 11 that represents results of such processing. Here the behavior of the data is similar to that in Fig. 8 where we also observe adequate generalization of results except for the region of low Rayleigh numbers and with large channel lengths. This region of thermogravitational convection has some special features and requires special consideration. This implication is supported by conclusions of [11].

CONCLUSIONS

We have represented results of the numerical investigation of the flow and heat transfer between two isothermal vertical plates under laminar natural convection. The calculations were performed in a wide range of Rayleigh number $\mathrm{Ra} = 10 \div 10^5$ and relative channel length $\mathrm{AR} = L/w = 1 \div 500$. We have analyzed the effect of these parameters on the gas-dynamic and thermal structure of thermogravitational convection, the local and mean heat transfer, and also on the gas flow rate between the plates (convective draft).

We have found the ranges of the regions and regime parameters when the local heat flux on the walls tends to zero due approach of the gas temperature to surface temperature. It has been shown that the mean heat transfer decreases as the relative channel length AR grows whereas the integral gas flow rate (convective draft) and the Reynolds number in the channel, $\mathrm{Re} = 2wUm/\nu$, grow.

The use of the modified Rayleigh number $\mathrm{Ra}^* = \mathrm{Ra} \cdot (w/L)$ results in generalization of the calculation data on mean heat transfer. These data are in good agreement with the correlations for heat transfer [1, 2] and gas flow rate [3]. The cases of low Rayleigh numbers when the asymptotic behavior of the heat transfer coefficient is observed are the only exception. Similarly looks the data representation in the form of integral heat transfer versus modified Reynolds number.

NOTATIONS

$\mathrm{AR} = L/w$—aspect ratio
L—channel height
w—spacing between plates, mm
$\mathrm{Nu} = 2\alpha w/\lambda$—Nusselt number
$\mathrm{Ra} = g\beta(T_0 - T_w)w^3/a\nu$—Rayleigh number
$\mathrm{Ra}' = Raw/L$—modified Rayleigh number
$\mathrm{Re} = 2Um \cdot w/\nu$—Reynolds number
x, y—longitudinal and vertical coordinates, mm
U_m—bulk velocity in the channel, m/s
α—heat transfer coefficient, W/(m^2·K)
λ—thermal conductivity coefficient, W/(m·K)
ν—kinematic viscosity, m^2/s
ρ—density, kg/m^3

ACKNOWLEDGMENTS

This work was supported by the Russian Science Foundation, project no. 14-19-00402.

REFERENCES

1. Elenbaas, W., Heat Dissipation of Parallel Plates by Free Convection, *Physica*, 1942, vol. 9, no. 1, pp. 2–28.
2. Bar-Cohen, A. and Rohsenow, W.M., Thermally Optimum Spacing of Vertical, Natural Convection Cooled, Parallel Plates, *J. Heat Transfer*, 1984, vol. 106, pp. 116–123.
3. Olsson, C.-O., Prediction of Nusselt Number and Flow Rate of Buoyancy Driven Flow between Vertical Parallel Plates, *J. Heat Transfer*, 2004, vol. 126, pp. 97–104.
4. Bodoia, J.R. and Osterle, J.F., The Development of Free Convection between Heated Vertical Plates, *J. Heat Transfer*, 1962, vol. 84, pp. 40–44.
5. Sparrow, E.M., Chrysler, G.M., and Azevedo, L.F., Observed Flow Reversals and Measured Predicted Nusselt Numbers for Natural Convection in a One Sided Heated Vertical Channel, *J. Heat Transfer*, 1984, vol. 104, no. 2, pp. 325–332.
6. Elenbaas, W., The Dissipation of Heat by Free Convection: The Inner Surface of Vertical Tubes of Different Shapes of Cross-Section, *Physica*, 1942, vol. 9, no. 8, pp. 865–874.
7. Campo, A., Manca, O., and Morrone, B., Numerical Investigation of the Natural Convection Flows for Low-Prandtl Fluids in Vertical Parallel-Plates Channels, *J. Appl. Mech.*, 2006, vol. 73, pp. 96–107.
8. Lau, G.E., Timchenko, V., Menezo, C., et al., Numerical and Experimental Investigation of Unsteady Natural Convection in a Vertical Open-Ended Channel, *Comp. Therm. Sci.*, 2012, vol. 4, iss. 5. pp. 443-456, DOI: 10.1615/ComputThermalScien.2012005217.
9. Roeleveld, D., Naylor, D., and Oosthuizen, P.H., Empirical Correlation for Free Convection in an Isothermal Asymmetrically Heated Vertical Channel, *Heat Trans. Eng.*, 2009, vol. 30, pp. 189–196.
10. Aung, W., Fully Developed Laminar Free Convection between Vertical Plates Heated Asymmetrically, *Int. J. Heat Mass Transfer*, 1972, vol. 15, pp. 1577–1580.
11. Terekhov, V.I. and Ekaid, A.L., Turbulent Free Convection between Vertical Isothermal Plates with Asymmetrical Heating, *Therm. Aeromech.*, 2013, vol. 20, no. 2, pp. 151–162.
12. Terekhov, V.I. and Ekaid, A.L., Laminar Natural Convection between Vertical Isothermal Plates with Different Temperatures, *J. Eng. Therm.*, 2011, vol. 20, no. 4, pp. 416–433.
13. Martin, L., Raithby, G.D., and Yovanovich, M.M., On the Low Rayleigh Number Asymptote for Natural Convection through an Isothermal Parallel-Plate Channel, *J. Heat Transfer*, 1991, vol. 113, pp. 899–905.
14. Patankar, S., *Numerical Heat Transfer and Fluid Flow*, Washington: Hemisphere, 1980.
15. Ekaid, A.L., Chichindaev, A.V., and Terekhov, V.I., Laminar Natural Convection between Vertical Isothermal Plates with Different Temperatures, *Proc. 7th Int. Conf. on Computational Heat and Mass Transfer*, Istanbul, 2011, no. 185.
16. Ekaid, A.L., Numerical Investigation of Free Convection Heat Transfer in Open and Clouse Enclosures, Ph. D. Thesis, Novosibirsk, 2013.
17. Shah, R.K. and London, A.L., Laminar Flow Forced Convection in Ducts, in *Adv. Heat Transfer*, suppl. 1, New York: Academic Press, 1978.